Hexacoordination of Bacteriochlorophyll in Photosynthetic Antenna LH1†

Leszek Fiedor*

Faculty of Biotechnology, Jagiellonian University, Gronostajowa 7, 30-387 Cracow, Poland

Received July 19, 2005; Revised Manuscript Received December 9, 2005

ABSTRACT: The ability of chlorophylls to coordinate ligands is of fundamental structural importance for photosynthetic pigment−protein complexes, where in virtually all cases the pigment is thought to be in a pentacoordinated state. In this study, the correlation of the Q_X transition energy with the coordination state of the central metal in bacteriochlorophyll is applied in investigating the pigment coordination state in bacterial photosynthetic antenna LH1. To facilitate a detailed spectral analysis in the Q_X region, carotenoid-depleted forms of LH1 are prepared and model LH1 are constructed with non-native carotenoids having blue-shifted absorption. The deconvolution of the Q_X envelope in LH1 reveals that the band is the sum of two transitions, which peak near 590 and 607 nm, showing that a significant fraction (up to 25%) of hexacoordinated bacteriochlorophyll is present in the complex. The hexacoordination can be seen also in LH1 antennae from other species of purple photosynthetic bacteria. It seems correlated with the LH1 aggregation state and probably is a consequence of the structural flexibility of the assembled complex. The sixth ligand probably originates from the apoprotein and seems not to affect the chromophore core size. These findings show that in light-harvesting complexes a hexacoordinated state of bacteriochlorophyll is not uncommon. Its presence may be relevant to a correct assembly of the antenna and have functional consequences, as it results in a splitting of the pigment S_2 excited state (Q_X), i.e., the carotenoid excitation acceptor state, what might affect intracomplex carotenoid-to-bacteriochlorophyll energy transfer.

Chlorophylls (Chls),[1] being the key cofactors of all primary photosynthetic processes, are indispensable for photosynthesis (*1*). They are designed by nature in such a way that their conjugated π-electron system (see the structure of bacteriochlorophyll *a* in Figure 1) can be shaped via various interactions with their environment (*2*). Hence, photophysical and redox properties of Chls in vivo are tuned such that they either mediate photon capturing and convey the excitation energy in the light-harvesting (LH) complexes or support electron transfer in reaction centers, carrying out the conversion of light energy into biologically useful chemical energy (*1*).

From many biochemical and spectroscopic studies (*3*−*9*) and from the increasing number of available high-resolution structures of photosynthetic pigment−protein complexes (*10*−*17*), it is apparent that Chls are also important structural cofactors, essential for the assembly of these complexes in photosynthetic membranes. In LH complexes, their structural function relies in large part on the ability of the central metal ion (in most cases Mg^{2+}) to coordinatively interact with amino acid residues (*11*, *12*, *18*−*20*). However, coordination to the central metal ions in the special pair bacteriochlorophyll (BChl) is not required in reaction centers (*21*).

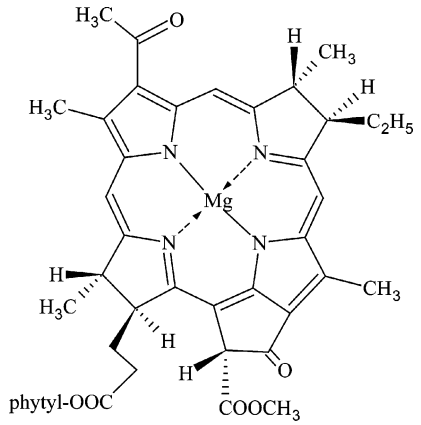

FIGURE 1: Structural formula of BChla. The arrows indicate two (formally) coordinative bonds to the central Mg ion.

The properties of the central Mg^{2+} ion, its exchange, and other reactions in plant and bacterial Chls have long been a subject of extensive studies (*22*−*28*). The chelation of central Mg by tetrapyrrolic nitrogens does not satisfy the metal coordination sphere, and thus, additional axial ligands are readily coordinated (*29*). In fact, the ligand-free form of (B)Chl is virtually nonexistent; in most solvents, the preferred coordination number of the central Mg is five, while energetically less favorable hexacoordination is well documented as existing only in strongly coordinating solvents, such as pyridine (*29*−*31*). Even in neat noncoordinating solvents, (B)Chl tends to coordinate either another pigment molecule [aggregation (*32*)] or nucleophilic trace impurities, e.g., residual water molecules, as axial ligands (*33*, *34*).

In biological systems, hexacoordination of Mg in Chls is found only rarely, if at all; in virtually all photosynthetic

† The project was supported by the Volkswagen Foundation (Grant I/77 876) and by the Polish Ministry of Science (KBN Project 6 P04B 00321).

* To whom correspondence should be addressed. Telephone: ++48-12-6646358. Fax: ++48-12-6646902. E-mail: lfiedor@mol.uj.edu.pl.

[1] Abbreviations: BChl, bacteriochlorophyll; Chl, chlorophyll; β-OG, *n*-octyl β-glucopyranoside; Crt, carotenoid; fwhm, full width at half-maximum; LDAO, *N*,*N*-dimethyldodecylamine *N*-oxide; LH, light-harvesting; Lyc, lycopene; Neu, neurosporene; RR, resonance Raman; Sph, spheroidene; Spx, spirilloxanthin; WT, wild-type.

10.1021/bi0514055 CCC: $33.50
Published on Web 01/20/2006

complexes of known structures, pentacoordination is seen (*35*, *36*). Therefore, it was intriguing to find indications of two populations of differently ligated BChla in the absorption spectrum of LH1 from *Rhodospirillum rubrum*. The π-electron system of (B)Chls is sensitive to the changes in partial charge density in the central metal ion, manifested as shifts in their redox potentials and electronic transitions, induced by the metal exchange and coordination of axial ligands (*27*, *30*, *31*, *34*, *37*, *38*). The Q_X transition in BChla, particularly prone to such effects, can be used as an indicator of the coordination state of the pigment (*27*, *31*). At present, this approach has been applied in investigating the coordination state of BChl in bacterial photosynthetic antenna LH1. The analysis of the Q_X band shape, based on deconvolution, shows that all BChla molecules are monoligated in the subunits of LH1, whereas it reveals a significant fraction of biligated BChla in fully assembled native and reconstituted LH1. The presence of two coordinational forms of BChla has structural consequences and possibly also consequences for the functioning of the bacterial light-harvesting complexes.

EXPERIMENTAL PROCEDURES

BChla Isolation. Bacteriochlorophyll *a* (BChla) was extracted with methanol from lyophilized cells of carotenoid-less strain R-26.1 of *Rhodobacter sphaeroides* and purified by column chromatography on DEAE-Sepharose CL-6B (Pharmacia, Uppsala, Sweden), according to a published method (*39*). The final step of purification was done by isocratic HPLC on silica gel, as previously described (*40*, *41*). The purified pigment was stored under Ar at −30 °C in the dark.

B820 Isolation. The B820 subunits of LH1 were obtained via a controlled detergent solubilization of lyophilized, benzene-extracted, bacterial photosynthetic membranes (chromatophores) from wild-type *Rsp. rubrum* (S1 strain). The subunits were purified by ion exchange column chromatography on DEAE-Sepharose CL-6B FastFlow (Pharmacia) in the presence of 1% β-OG, as described by Fiedor and Scheer (*42*). If necessary, the chromatographic step was repeated.

B780 Formation. The B780 subform of LH1 was prepared by titration of the B820 subunit at room temperature with 20% β-OG (w/v), until a complete dissociation was achieved (final β-OG concentration of 4%). The progress of dissociation was monitored by absorption spectroscopy.

B870 Formation. The B870 complex was obtained from a purified B820 subunit by a 2-fold dilution with a cold Tris-HCl buffer (10 mM, pH 7.6). The absorption spectrum of the sample was recorded after several minutes and then after 6 h at 4 °C in the dark.

Isolation of Native LH1. The native LH1 complex was obtained from chromatophores of *Rsp. rubrum* S1 by a modification of the method of Picorel et al. (*43*), as described previously (*44*).

Reconstitution of LH1 with Non-Native Carotenoids. The replacement of spirilloxanthin in LH1 from *Rsp. rubrum* with neurosporene and spheroidene was done using the reconstitution method described by Fiedor et al. (*44*).

Absorption and Emission Measurements. The absorption spectra were measured at room temperature in a 1 cm quartz cuvette on a Cary 50 (Varian) spectrophotometer, applying a 0.5 nm increment and a 0.2 s integration time per point. The fluorescence excitation spectrum of the LH1 complex was recorded at room temperature in a 1 cm quartz cell, on a Spex fluorolog 1680 spectrofluorimeter, equipped with 0.22 m double monochromators.

Spectral Deconvolution. The spectral deconvolution was performed according to a method described by Kania and Fiedor (*45*). The wavelength scale in the absorption spectra was converted to the linear energetic scale (inverse centimeters), and the spectra were analyzed using version 4.0 of PeakFit (Jandel). The deconvolution was performed without any smoothing, any filtering, or any other data pretreatment. During the analyses in all cases the same criteria were applied: (1) A uniform type of all components was used. (2) The number of envelope components was kept to a minimum. (3) The energies of the 0−1 and 0−2 vibrational sidebands of the Q_X transition were placed 1000−1200 cm^{-1} higher than their origin (only solutions resulting in sidebands of intensities near 20−30% of origin intensity were accepted). (4) To partly compensate for the contributions of the Soret and Q_Y bands, prior to deconvolution, a background subtraction was carried out, always using a similar flat quadratic curve, centered near 17 000 cm^{-1}. If necessary, Crt absorption bands were also included in the deconvolution.

RESULTS

Electronic absorption spectra of isolated BChla in organic solvent dimethylformamide (DMF) and the one located within photosynthetic proteins, viz. subforms of the LH1 complex and fully assembled LH1 (with and without Crts), are shown in Figure 2. There is a great variability in Q_Y transition energies among these forms of BChla, whereas their other bands, Soret and Q_X, seem much less affected. This is due to the well-known sensitivity of the Q_Y transition to the pigment aggregation state (*32*, *46*). It is located between 770 and 800 nm in the monomeric form, between 820 and 860 nm in the dimeric states (*5*, *32*, *46*, *47*), and between 850 and 963 nm in larger arrays, such as fully assembled LH complexes (*4*, *48*). The Q_X band shows a much weaker dependence on the pigment situation, as seen in Figure 3, where the expanded Q_X regions of the spectra from Figure 2 are presented.

BChla in Coordinating Organic Solvent. The position of the Q_Y transition of BChla in neat DMF at 770 nm (Figure 2A) indicates the monomeric state of the pigment in that solvent. The Q_X band of BChla in DMF is very broad and clearly asymmetric (Figure 3A), comprising at least two closely located transitions of uneven intensities, the stronger one centered near 580 nm and the weaker one near 610 nm.

BChla in Carotenoid-less LH1 and Its Subforms. The B820 subunit (Figure 2A) was obtained by the treatment of carotenoid-devoid chromatophores from WT *Rsp. rubrum* with 3.4% β-OG and purified by ion exchange chromatography in the presence of 1% β-OG. Fully aggregated LH1 and its B780 subform (absorption spectra shown in Figure 2A) were both obtained from purified B820 subunits, by adjusting the β-OG concentration. By lowering its concentration to $<0.5\%$, the aggregation state of BChla changes from dimeric in B820 to fully aggregated in B870. The increase in the detergent concentration to 4% causes the dissociation of B820 and yields the monomeric form, B780.

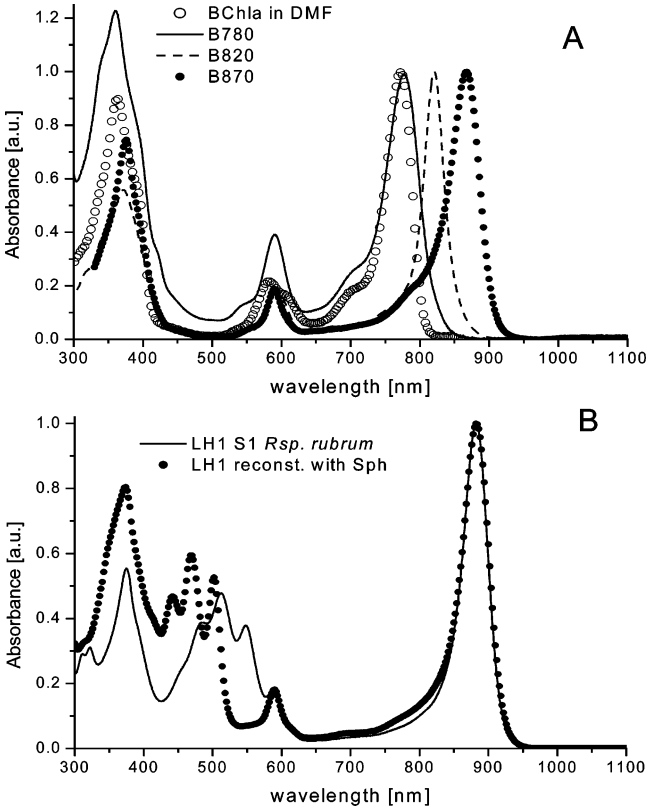

FIGURE 2: Absorption spectra of (A) BChla in dimethylformamide, and in various forms of carotenoid-depleted LH1 complex (B780, B820, and B870) from *Rsp. rubrum*; and (B) native LH1 from *Rsp. rubrum* and LH1 reconstituted with spheroidene. The spectra were normalized to match the intensities of the most red-shifted transition (Q_Y) of BChla.

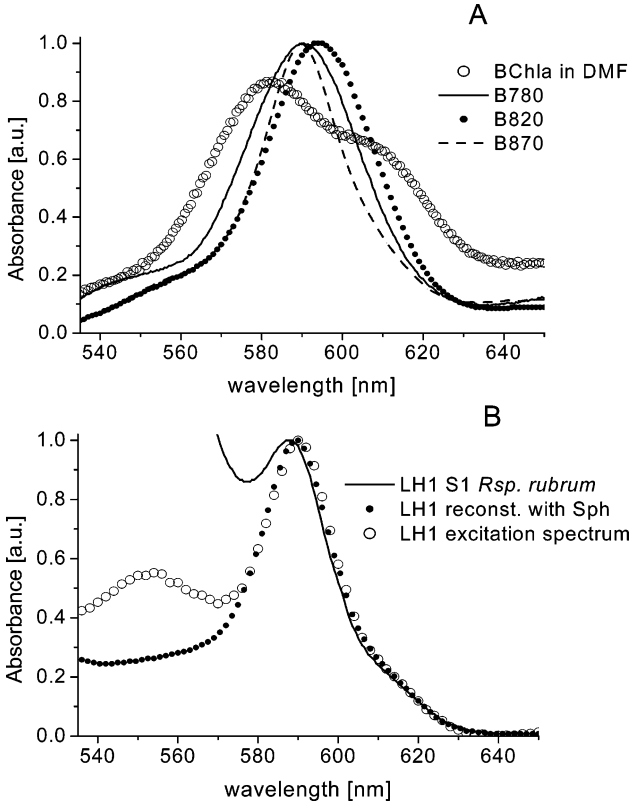

FIGURE 3: Expanded Q_X regions (of the spectra from Figure 2) of (A) BChla in dimethylformamide and various forms of carotenoid-depleted LH1 complex (B780, B820, and B870) from *Rsp. rubrum*; and (B) native LH1 from *Rsp. rubrum* and LH1 reconstituted with spheroidene. For clarity, the spectra in the top panel were normalized by a factor to bring the Q_X band intensities near a value of 1; the spectra in the bottom panel were normalized to the Q_X band.

The position of the Q_X band of BChla in the three forms of the Crt-devoid LH1 complex shifts slightly with the pigment aggregation state (from 590 to 595 nm on going from B870 to the B820 subform), and in B780 it moves back to the original position (Figure 3A). Also, the Q_X bandwidth shows some dependence on the pigment aggregation state; the band is narrow in B870, while in B820 and in particular in B780, it becomes considerably broader (Figure 3A).

BChla in Carotenoid-Containing LH1 Complexes. The absorption spectra of BChla located within the Crt−polypeptide environment of the LH1 complex from *Rsp. rubrum* are shown in Figure 2B. The LH1 complexes have been prepared with three different Crts: spirilloxanthin (Spx, 13 conjugated C═C bonds), spheroidene (Sph, 10 conjugated C═C bonds), and neurosporene (Neu, 9 conjugated C═C bonds). The native LH1 complex, containing mostly Spx (*49*), was isolated from chromatophores of wild-type *Rsp. rubrum* (S1), while the complexes with the two non-native Crts were obtained via a recently developed reconstitution technique (*44*). In native LH1, the Spx absorption overlaps with the BChl Q_X transition but the replacement of Spx with Sph or Neu yields LH1 complexes with blue-shifted Crt absorption (Figure 2B). As seen in Figure 3B, in the LH1 reconstituted with Sph there is a clear asymmetry in the shape of the Q_X band; next to the main transition (λ_{max} = 589 nm), a weaker shoulder extends up to 630 nm. The Q_X band profile in LH1 reconstituted with Neu exhibits an identical feature (not shown).

The fluorescence excitation spectrum of native LH1, presented in Figure 3B, was determined in the region of the Q_X absorption by monitoring the emission from LH1 at 900 nm. It coincides perfectly with the Q_X absorption band of LH1 reconstituted with Sph, including the shoulder on the low-energy side. The other weaker band seen in the excitation profile, located near 550 nm, corresponds to the 0 → 0 transition in Spx (*50*) and reflects the low efficiency of excitation energy transfer from Spx to LH1 BChl in the wild-type complex (*51*).

Q_X Band Deconvolution. To resolve the component transitions of the Q_X absorption band of BChla in solution and in LH complexes, respective fragments of the absorption spectra (shown in Figure 3) were plotted in the energy (linear) scale and subjected to deconvolution following a method recently applied to determination of thermodynamic parameters and steric factors in ligation of bacteriochlorophyll *a* in organic solvents (*45*). Also for BChla bound in LH complexes, the best fits to the Q_X envelope were obtained assuming Gaussian−Lorentzian-type components, in accordance with the results reported by Umetsu et al. (*52*). The sums of the Gaussian−Lorentzian components gave an almost perfect overlap with the experimental curves, as shown in Figure 4, typically yielding values for the coefficients of determination (r^2) higher than 0.999. Gaussian or Voigt functions, which are often used for fitting of Chl and BChl spectra (usually in the Q_Y region) (*53*, *54*), not only resulted in lower values of the r^2 parameter but also required a larger number of components to be taken into account for adequate fitting of the Q_X band (not shown). Moreover, while

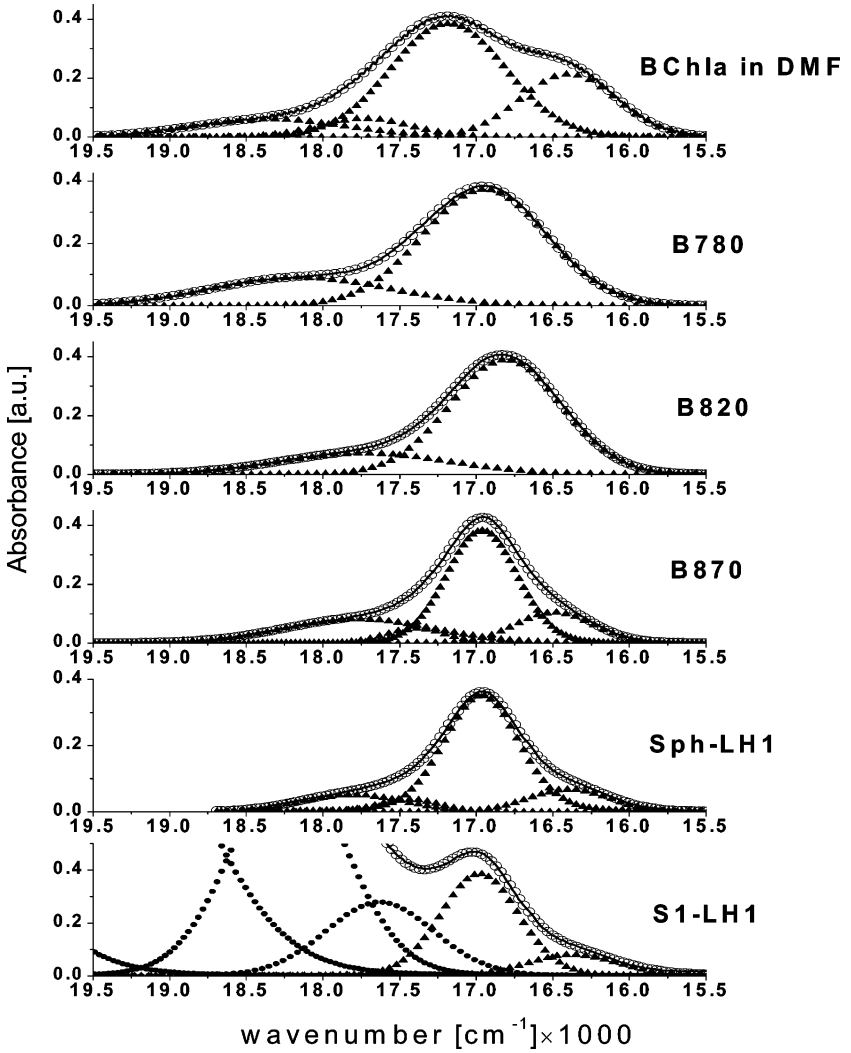

FIGURE 4: Gaussian−Lorentzian deconvolution (see the text for details) of the Q_X region of the absorption spectra of BChla in various environments: in dimethylformamide, in carotenoid-less LH1 antenna in different states of aggregation (monomeric B780, dimeric B820, and fully aggregated B870), and in LH1 complexes [reconstituted with spheroidene (Sph−LH1) and native, containing mainly spirilloxanthin (S1−LH1)]. Experimental data are shown as a solid line; fitted components are marked with black triangles (BChla transitions) and black circles (carotenoid bands); the sums of the deconvolution components are marked with white circles.

applying the Gaussian−Lorentzian components, in many instances the deconvolution algorithm was itself able to eliminate redundant components. As reviewed by Zucchelli et al. (*55*), the complex, Gaussian−Lorentzian, character of the Q_X band components stems from the fact that in principle the band shape of these electronic transitions can be described as a Lorentzian function with a considerable Gaussian "dress", arising due to the statistical broadening (the inhomogeneous contribution).

The results of deconvolution in LH1 complexes are plotted in Figure 4, and the relevant deconvolution parameters are summarized in Tables 1 and 2. The analysis of the Q_X envelopes in all cases resolved well the main (0−0) Q_X transition with its vibrational sidebands (the bands centered above 17 500 cm^{-1}). The positions of the vibrational sidebands, relative to the 0−0 transition, were estimated on the basis of the measurements of BChla spectra in acetone and pyridine, in which single coordinative forms of the pigment are present [i.e., pentacoordination in acetone and hexacoordination in pyridine (*45*)]. Further discussion is focused primarily on the 0−0 transitions, with the maxima located below 17 200 cm^{-1}, as these are directly correlated with the coordination state of the central Mg in BChla (*2*, *31*, *45*, *52*). The intensities of the component transition are given in terms of their contribution to the total band intensity (sum of the areas of all contributing Q_X transitions).

Table 1: Deconvolution of the Q_X Band in Various Forms of BChla

BChla form, experimental values[a]	band	λ_{max}[a]	fwhm (cm^{-1})	%
DMF, 17212, 581	1	16397, 610	738	32
	2	17182, 582	877	68
	3	17727, 564	706	−
	4	18345, 545	1176	
B780, 16935, 591	1	16941, 590	954	100
	2	18146, 551	1359	−
B820, 16835, 594	1	16807, 595	857	100
	2	17732, 564	1292	−
B870, 16920, 591	1	16489, 606	594	23
	2	16962, 590	545	77
	3	17303, 569	454	−
	4	17766, 563	1145	

[a] The first value is given in inverse centimeters and the second in nanometers.

Monomeric BChla in a Coordinating Organic Solvent. The nonsymmetric Q_X band of BChla in DMF could be fitted

Table 2: Deconvolution of the Q_X Band in the Native LH1 Complex from *Rsp. rubrum* and LH1 Reconstituted with Spheroidene and Neurosporene

LH1 complex, experimental values[a]	band	λ_{max}[a]	fwhm (cm^{-1})	%
native (S1), 17007, 588	1	16368, 611	690	19
	2	16976, 589	598	81
	3	17628, 567	831	–
	4	18220, 549	860	
	5	19436, 515	1350	
Sph, 16945, 590	1	16393, 610	620	17
	2	16964, 589	576	83
	3	17440, 573	470	–
	4	17805, 562	793	
Neu, 16978, 589	1	16603, 602	650	24
	2	16997, 589	506	76
	3	17397, 575	434	–
	4	17819, 561	854	

[a] The first value is given in inverse centimeters and the second in nanometers.

very well with the minimal number of two Gaussian−Lorentzian components (Figure 4), a stronger one centered near 17 180 cm^{-1} and a weaker one near 16 400 cm^{-1}. The ratio of their intensities was found to be equal to 3:1 (Table 1).

LH1 Complex and Its Subunit Forms. Deconvolution in the monomeric (B780) and dimeric (B820) subforms of LH1 reveals strictly single Gaussian−Lorentzian components under the Q_X band (Figure 4), with the maxima at 16 940 and 16 800 cm^{-1}, respectively (Table 1). A treatment of these two subforms with up to 2 M imidazole had no effect on the shape (and results of deconvolution) of the Q_X band (see the Supporting Information). In fully aggregated B870, deconvolution gives a satisfactory result (Figure 4) only if, next to the main component at 16 962 cm^{-1}, another minor transition is included, centered near 16 490 cm^{-1}, which constitutes 23% of the entire band (Table 1).

Deconvolution in the LH1 complexes reconstituted with Sph (Figure 4) and Neu (not shown) did not require consideration of Crt absorption. It gives a pattern very similar to the one in B870; there are two Q_X components, and their contributions to total band intensity are equal to 17 and 24% (Table 2). Deconvolution in the native LH1 antenna is slightly less reliable, because it included Crt transitions. Nevertheless, here also, to obtain a good fit, two components under the Q_X band had to be assumed, with intensities in a ratio of 4:1 (Table 2). In addition, the presence of a shoulder on the low-energy side of the Q_X band is also evident in the LH1 fluorescence excitation profile (Figure 3B).

Width of the Q_X Transitions. A comparison of the deconvolution results shows that the Q_X envelopes of BChla in various environments resolved into components (Tables 1 and 2) of significantly varying full width at half-maximum (fwhm). The component transitions are considerably broader for BChla in DMF, B780, and B820 (Table 1) than in B870 and in the assembled LH1 (Table 2). The component located near 17 000 cm^{-1} in the monomeric (DMF and B780) and dimeric pigment (B820) forms has fwhms equal to 877, 954, and 857 cm^{-1}, respectively. In all analyzed LH1 complexes, including B870, the higher-energy components are considerably narrower and their fwhms do not exceed 600 cm^{-1}.

The lower-energy (16400−16600 cm^{-1}) component of the Q_X band shows a similar dependence on the location of the chromophore: it is again relatively broad in DMF (fwhm = 700 cm^{-1}) and becomes quite narrow, near 500 cm^{-1}, in LH1 complexes.

DISCUSSION

BChla is perhaps one of the best examples for which the coordination state of the central metal ion can be inferred directly from the energy of the Q_X transition (*27*, *30*, *31*). When the central Mg ion in BChla is pentacoordinated (one axial ligand), the Q_X transition peaks between 17 500 and 16 950 cm^{-1} (570−590 nm), while in the hexacoordinated one (two axial ligands), it shifts below 16 600 cm^{-1} (above 600 nm). On the other hand, as seen in Figures 2 and 3, the Q_X band energy is practically insensitive to the aggregation state of the pigment, both in vitro and in vivo (*5*, *46*, *47*), and hence, the correlation of the band shift with the central Mg coordination state applies also in vivo (*52*).

BChla in a Coordinating Solvent. Applying the criteria established by Callahan and Cotton (*31*), we find the splitting of the Q_X band of BChla in relatively strongly coordinating DMF is rather straightforward to interpret. The observed band shape in DMF is the sum (envelope) of two components (transitions) which correspond to two species of BChla, being in equilibrium with each other in solution: the pentacoordinated (higher-energy component) and hexacoordinated (lower-energy component) forms. The equilibrium between the two coordination forms strongly depends on temperature (*45*) (see the Supporting Information).

Coordination State of BChl in the LH1 Antenna. In both subforms of LH1, B780 and B820, deconvolution shows the presence of only single symmetric Q_X transitions ($\lambda_{max} \sim$ 590 nm), and therefore, BChls in the two subforms seem exclusively monoligated. This is in accordance with other spectroscopic studies showing BChla in B820 and in B780 to be monoligated by His residues from the α- and β-polypeptides (*5*, *18*). A different, two-component deconvolution pattern has been found in the fully assembled B870 complex from *Rsp. rubrum*, both the native and reconstituted, with the lower-energy transition constituting up to 25% of the major one. Thus, according to band energy criteria, ∼75−80% of BChls in LH1 seem monoligated while the remaining fraction should be classified as biligated. The presence of the minor fraction is also evident from the excitation spectrum of the complex, at the same time confirming an efficient energetic coupling of the minor Q_X transition to the B880 BChls. A closer examination of the LH1 absorption profiles found in the literature reveals that even without spectral deconvolution this minor transition can be seen also in LH1 complexes from other species of purple photosynthetic bacteria (*56*−*59*) as well as in the RC−LH1 complexes, e.g., from *Rhodobium marinum* and *Rb. sphaeroides* (*60*−*62*).

As mentioned before, the coordination number 6 of the central Mg is rather uncommon to (B)Chls in in vivo systems (*35*, *36*), and even in solution, it can be found only in highly coordinating media (*31*). However, it is difficult to suggest another plausible explanation for the presence of this lower-energy component in LH complexes. For instance, the excitonic interactions between the members of the B880 ring could be considered in LH1, but the Q_X band is practically insensitive to the aggregation. Moreover, such effects are

not observed in other systems of strongly coupled BChls, B820 and B850. Second, the excitonic interactions, in parallel to the shifts in the absorption, are expected to give rise to signals in circular dichroism spectra, actually not observed in that region (*5*, *44*, *59*). On the other hand, the BChl distortions are also very unlikely to be the reason for the observed splitting of the Q_X band in LH1. First, the ring distortions are expected to affect mostly the Q_Y transition (*63*), but no indication of shoulders or asymmetry of the lowest-energy absorption band of LH1 is seen (Figure 2B). Moreover, any significant change in ring distortions on going from the B780 and B820 forms to B870 would have been readily detected using the resonance Raman (RR) technique, which seems not to be the case (*5*, *64*). The RR measurements exhibited a similar, conserved type of distortion of the pigment macrocycle in both LH1 and LH2 antennae, if compared to a more relaxed conformation of BChl in organic solvents (*64*). Finally, the out-of-plane displacement of the central Mg induced by BChla−polypeptide interactions within LH1 cannot be the reason either as it is known to cause a shift of the Q_X position to 570−590 nm (∼17 000 cm^{-1}); the shift above 600 nm (16 700 cm^{-1}) is usually correlated with the in-plane placement of the central ion (*31*, *65*, *66*). Such displacements would be also expected to be seen using RR spectroscopy (see below).

The interactions of BChls in solution and within LH complexes have been extensively studied using many techniques, including RR spectroscopy (*5*, *31*, *64*−*67*). In particular, the lowering of vibrational frequencies of bands A and B [the C_aC_m and C_aC_b stretchings, respectively (*65*)] from 1609/1530 to 1589/1512 cm^{-1} is consistent with the core expansion caused by the movement of the central Mg into the plane of the macrocycle upon binding of the second axial ligand. The RR experiments performed on the LH1 antenna and its subunits, isolated from *Rsp. rubrum*, do not reveal these characteristic shifts of the BChla Raman bands, thus indicating the same coordination state 5 of the pigment in all forms of the complex (*5*, *64*). With regard to the fully assembled complex, this result though is inconsistent with the present assignment of a population of six-coordinated BChla in LH1, based on absorption spectroscopy.

Considering differences in the physical principles underlying the two spectroscopic techniques, a straightforward explanation of this apparent inconsistency can be suggested. In a series of metallo-substituted BChls, it was shown that the frequencies of the coordination-sensitive Raman modes are not directly dependent on the coordination state of the central metal but rather on the size of the pigment core (*68*). Hence, the results of the RR measurements on LH1 and the subunits do not necessarily confirm the chromophore pentacoordination but may in fact indicate that there are no significant changes in the BChl core size in B780, B820, and B870. This could possibly take place, for instance, when in a polypeptide-bound BChla, the position of the central ion with respect to the macrocycle (and CC stretchings) is similar (or constant) along the series of LH1 forms, implying an exceptionally strong binding of the pigment to the apoprotein. There are several indications of indeed a strong mode of binding of BChla in LH1 and its subunits, such as a considerably red-shifted position (590−595 nm) of the Q_X transition (Table 1) with respect to coordinating solvents [a similar shift is observed only in pyridine (*27*)]. A strong coordination of BChls by apoproteins seems to be a common feature of various bacterial LH complexes, both LH1 and LH2 (*18*, *20*).

Another indication of the strong coordination of BChl is its inaccessibility in B780 and B820 to external ligands, such as a strongly coordinating imidazole. While in the case of B820 the central Mg might not be "visible" to external ligands due to the dimerization and steric crowding in the $(BChla)_2$-$\alpha\beta$ heterodimer, the same argument does not apply after the interactions stabilizing the heterodimer are disrupted due to the detergent treatment (4% β-OG), resulting in a complete dissociation to monomeric form B780. Nevertheless, the His−BChla coordination bond remains intact in B780 (*18*), and even in the presence of 2 M imidazole (6 order of magnitude molar excess), there are no signs of hexacoordination (see the Supporting Information). Seemingly, the out-of-plane position of the central Mg (*66*) is somehow stabilized due to the binding to the polypeptides. Assuming such freezing of BChla conformation in LH1, the interactions with any electron-rich center (ligand) located in the axial position in the vicinity of the polypeptide-bound BChla would lead to changes in the partial charge density on the central ion, without affecting its position with respect to the macrocycle. It has been shown that binding of axial ligands to (B)Chls significantly affects the charge density on the central metal, and in particular, the energy of the Q_X transition in BChla is sensitive to these changes (*27*, *69*). In this context, the absorption spectroscopy seems to be a more direct means for monitoring interactions between the central metal and the chromophore π-electron system which are related to the coordination.

Following the reasoning given above, we can attribute the presence of the red-shifted Q_X transition in LH1 to a fraction of BChla which seems to be involved in an unusual mode of hexacoordination, occurring without a detectable pigment core expansion. Consequently, the position of the red Q_X transition in LH1 below 610 nm suggests the extra ligand is bound via O rather than through N (*31*). Furthermore, the measurements of the temperature-induced changes in the absorption spectra (data shown in the Supporting Information) show that in contrast to BChla in solution (DMF), both the position and intensity of the red-shifted Q_X band in the LH1 spectrum are invariable in the range between 0 and 20 °C. This indicates that a specific polar amino acid residue might be involved in the sixth ligand binding. A comparison of the amino acid sequences of the α- and β-polypeptides from *Rsp. rubrum* shows that in the α-polypeptide two polar residues, potential ligands, are present near the BChl binding site: Ser and Asn residues at +5 and +10 positions, respectively (with respect to the His_0 residue of the primary contact to BChl), both highly conserved among several LH1 antennae from purple bacteria (*20*). Both residues are expected to be coordinating; alcohols are known to be excellent ligands of (B)Chls in solution (*31*, *70*), whereas Asn was found to interact with the central Mg of BChla in photosynthetic complexes (*71*). Also, in a Ser−BChla model compound, where a Ser moiety replaces the phytyl side chain (*72*), the presence of polar functional groups (amino group and methyl-esterified carboxylic group) near the macrocycle strongly enhances hexacoordination of BChla in aqueous solution (*54*). According to a recently obtained solution structure of the α-polypeptide from wild-type *Rsp. rubrum*,

these residues are located in the terminal part of the α-helical hydrophobic transmembrane domain of the polypeptide, not far from the BChl binding site (*73*), and hence, they could probably be involved in interactions with the *β*-polypeptide-bound pigment. The low intensity of the red-shifted Q_X band shows that only a fraction of the BChla molecules is involved in hexacoordination in LH1, but that is in agreement with the structure of the core antenna, showing a high degree of heterogeneity among the B880 BChls (*74*). Moreover, the RR measurements also revealed the presence of a minor population of BChla molecules in LH1 from *Rsp. rubrum*, whose local environment is different from the one in which the majority of B870 BChls are found (*67*).

Apparently, the coordination state of BChl in LH1 is correlated with the aggregation state of the complex. Probably, during assembly, the subunits (which contain strictly only monoligated BChla) undergo a structural rearrangement which in turn facilitates a hexacoordination of a certain fraction of BChla molecules. Many biochemical (*19*) and in particular recent crystallographic studies (*75*−*77*) reveal that in particular LH1 from *Rsp. rubrum* has indeed more structural flexibility than most of the LH2 complexes (*11*, *12*) and shows a strong degree of inequivalency among B880 BChls (*74*). On the other hand, as the flexibility of the assembled complex is permitting the hexacoordination, the character of BChl binding sites changes too, as indicated by differences in the width of the Q_X transitions, which show a considerable dependence on the location of the chromophore (Tables 1 and 2). In organic solvent at room temperature, a relatively broad Q_X envelope is seen because a range of ligand−BChl and $(ligand)_2$−BChl complexes (where the ligand is DMF), each with a slightly different Q_X energy, exists. A comparably broad Q_X band in B820, and an even wider one in B780, seems to result from the differences in the α-His and *β*-His coordination to BChla and hence a slight difference in the Q_X maximum position. Finally, a considerable narrowing of the Q_X band in the assembled LH1 results most probably from the increased rigidity of the BChl binding site due to the aggregation, which leads to a narrower distribution of the transition energies. In this context, the width of the Q_X band can be regarded as a good indicator of the pigment−protein interactions, a more reliable one than the Q_Y transition, because it seems to be fairly insensitive to the pigment−pigment interactions.

Relevance of BChl Hexacoordination in LH Complexes. The existence of a fraction of hexacoordinated BChl in the core antenna seems to be a more general feature; however, in the absence of a detailed structure of the bacterial LH1 antenna, it is not easy to propose a specific structural significance of the hexacoordination of BChl. A recent model study of the assembly of LH1 from *Rsp. rubrum* with Zn-substituted BChla has shown that up to 90% of the native pigment can be exchanged for the modified one, but it fails to restore the red-shifted position of the Q_Y band in the reconstituted complex, where it exhibited a shift to only 854 nm instead of 873 nm (*78*). In contrast, the Q_Y band position in LH1 complexes from *Rb. sphaeroides*, reconstituted (up to 53%) with Ni-substituted BChla, was identical to that in native LH1, i.e., 875 nm (*59*). One of the major differences between these two metallo-substituted BChls is the inability to assume the hexacoordinated state in the case of Zn, which preferentially binds only one axial ligand (*27*). This suggests that the sixth ligand binding to BChl might be of some relevance to a correct assembly of the LH1 antennae.

The biligation of BChl in LH1 may have consequences for the Crt-to-BChl energy transfer as in light-harvesting complexes from purple bacteria, the Q_X transition of BChl has been predicted to be a very efficient acceptor state of Crt excitation (*79*). The reason is that both the spectral overlap of this transition with Crt emission (from the S_2 state) and its orientation are favorable for efficient coupling with the Crt transition dipole (*80*, *81*). The structural analysis of, for example, the LH2 complex from *Rhodopseudomonas acidophila*, also shows a favorable parallel arrangement of Crt molecules and the Q_X dipoles of both B850 BChls (*82*). As evidenced by femtosecond absorption measurements on several LH2 and LH1 antennae, the excitation transfer from the strongly allowed S_2 state of Crt to the S_2 state (Q_X) of BChl is indeed the major route (up to 75% contribution) of singlet Crt-to-BChl energy transfer in these complexes (*51*, *81*, *83*). The appearance of a satellite Q_X transition, near the main one in the LH1 complex, may have consequences for their functioning. The most obvious would be (i) an increase in the spectral overlap of BChl absorption with Crt S_2 emission and (ii) the broadening of the Q_X transition and a lowering of its mean energy (hence, a shallower excitation trap). Both effects are expected to bring an improvement in the efficiency of Crt-to-BChl energy transfer, which would be relevant mainly for Crts with conjugation lengths from 9 to 11, which have energies of their 1Bu states close to that of Q_X (*51*, *80*, *81*, *83*). It would be expected that the Crt−Q_X channel may significantly contribute to the high efficiency of the Crt-to-BChl energy transfer in the LH1 complex from *Rb. sphaeroides* (with mostly Sph).

SUPPORTING INFORMATION AVAILABLE

Effects of imidazole on the coordination state of bacteriochlorophyll in the B780 and B820 subunits of LH1 antenna and effects of temperature on the coordination state of bacteriochlorophyll in organic solvent (dimethylformamide) and in fully assembled LH1 antennae. This material is available free of charge via the Internet at http://pubs.acs.org.

REFERENCES

1. Scheer, H. (1991) *Chlorophylls*, CRC Press, Boca Raton, FL.
2. Hanson, L. K. (1991) Molecular orbital theory of monomer pigments, in *Chlorophylls* (Scheer, H., Ed.) pp 993−1012, CRC Press, Boca Raton, FL.
3. Robert, B., and Lutz, M. (1985) Structures of antenna complexes of several *Rhodospirillales* from their resonance Raman spectra, *Biochim. Biophys. Acta 807*, 10−23.
4. Parkes-Loach, P. S., Michalski, T. J., Bass, W. J., Smith, U., and Loach, P. A. (1990) Probing the bacteriochlorophyll binding site by reconstitution of the light-harvesting complex of *Rhodospirillum rubrum* with bacteriochlorophyll a analogues, *Biochemistry 29*, 2951−2960.
5. Chang, M. C., Callahan, P. M., Parkes-Loach, P. S., Cotton, T. M., and Loach, P. A. (1990) Spectroscopic characterization of the light-harvesting complex of *Rhodospirillum rubrum* and its structural subunit, *Biochemistry 29*, 421−429.
6. Scheer, H., and Struck, A. (1993) Bacterial reaction centers with modified tetrapyrrole chromophores, in *The Photosynthetic Reaction Center* (Deisenhofer, J., and Norris, J. R., Eds.) pp 157−192, Academic Press, San Diego.
7. Sturgis, J. N., Jirsakova, V., Reiss-Husson, F., Cogdell, R. J., and Robert, B. (1995) Structure and properties of the bacteriochloro-

phyll binding site in peripheral light-harvesting complexes of purple bacteria, *Biochemistry 34*, 517−523.
8. Davis, C. M., Parkes-Loach, P. S., Cook, C. K., Meadows, K. A., Bandilla, M., Scheer, H., and Loach, P. A. (1996) Comparison of the structural requirements for bacteriochlorophyll binding in the core light-harvesting complexes of *Rhodospirillum rubrum* and *Rhodobacter sphaeroides* using reconstitution methodology with bacteriochlorophyll analogs, *Biochemistry 35*, 3072−3084.
9. Yang, C., Kosemund, K., Cornet, C., and Paulsen, H. (1999) Exchange of pigment-binding amino acids in light-harvesting chlorophyll a/b protein, *Biochemistry 38*, 16205−16213.
10. Deisenhofer, J., and Norris, J. R. (1993) *The Photosynthetic Reaction Center*, Academic Press, San Diego.
11. McDermott, G., Prince, S. M., Freer, A. A., Hawthornthwaite-Lawless, A. M., Papiz, M. Z., Cogdell, R. J., and Isaacs, N. W. (1995) Crystal structure of an integral membrane light-harvesting complex from photosynthetic bacteria, *Nature 374*, 517−521.
12. Koepke, J., Hu, X., Muenke, C., Schulten, K., and Michel, H. (1996) The crystal structure of the light-harvesting complex II (B800−850) from *Rhodospirillum molischianum*, *Structure 4*, 581−597.
13. Jordan, P., Fromme, P., Witt, H. T., Klukas, O., Saenger, W., and Krauss, N. (2001) Three-dimensional structure of cyanobacterial photosystem I at 2.5 Å resolution, *Nature 411*, 909−917.
14. Byrdin, M., Jordan, P., Krauss, N., Fromme, P., Stehlik, D., and Schlodder, E. (2002) Light harvesting in photosystem I: Modeling based on the 2.5-Å structure of photosystem I from *Synechococcus elongatus*, *Biophys. J. 83*, 433−457.
15. Kamiya, N., and Shen, J.-R. (2003) Crystal structure of oxygen-evolving photosystem II from *Thermosynechococcus vulcanus* at 3.7-Å resolution, *Proc. Natl. Acad. Sci. U.S.A. 100*, 98−103.
16. Ben-Shem, A., Frolow, F., and Nelson, N. (2003) Crystal structure of plant photosystem I, *Nature 426*, 630−635.
17. Liu, Z., Yan, H., Wang, K., Kuang, T., Jiping, Z., Gui, L., An, X., and Chang, W. (2004) Crystal structure of spinach major light-harvesting complex at 2.72 Å resolution, *Nature 428*, 287−292.
18. Sturgis, J. N., and Robert, B. (1994) Thermodynamics of membrane polypeptide oligomerization in light-harvesting complexes and associated structural changes, *J. Mol. Biol. 238*, 445−454.
19. Loach, P. A., and Parkes-Loach, P. S. (1995) Structure−function relationships in core light-harvesting complexes (LHI) as determined by characterization of the structural subunit and by reconstitution experiments, in *Anoxygenic Photosynthetic Bacteria* (Blankenship, R. E., Madigan, M. T., and Bauer, C. E., Eds.) pp 437−471, Kluwer Academic Publishers, Dordrecht, The Netherlands.
20. Zuber, H., and Cogdell, R. J. (1995) Structure and organization of purple bacterial antenna complexes, in *Anoxygenic Photosynthetic Bacteria* (Blankenship, R. E., Madigan, M. T., and Bauer, C. E., Eds.) pp 315−348, Kluwer Academic Publishers, Dordrecht, The Netherlands.
21. Goldsmith, J. O., King, B., and Boxer, S. G. (1996) Mg coordination by amino acid side chains is not required for assembly and function of the special pair in bacterial photosynthetic reaction centers, *Biochemistry 35*, 2421−2428.
22. Schunck, E., and Marchlewski, L. (1894) Zur Chemie des Chlorophylls, *Liebigs Ann. Chem. 278*, 329−345.
23. Willstätter, R., and Stoll, A. (1913) *Untersuchungen über Chlorophyll*, Verlag von Julius Springer, Berlin.
24. Vernon, L. P., and Seely, G. R. (1966) *The Chlorophylls*, Academic Press, London.
25. Strell, M., and Urumow, T. (1977) Neue Methoden zur Einführung von Metallen in Chlorophyll-derivative, *Liebigs Ann. Chem.*, 970−974.
26. Hynninen, P. H. (1991) Chemistry of chlorophylls: Modifications, in *Chlorophylls* (Scheer, H., Ed.) pp 145−209, CRC Press, Boca Raton, FL.
27. Hartwich, G., Fiedor, L., Simonin, I., Cmiel, E., Schäfer, W., Noy, D., Scherz, A., and Scheer, H. (1998) Metal-Substituted Bacteriochlorophylls. 1. Preparation and influence of metal and coordination on spectra, *J. Am. Chem. Soc. 120*, 3675−3683.
28. Noy, D., Fiedor, L., Hartwich, G., Scheer, H., and Scherz, A. (1998) Metal-substituted bacteriochlorophylls. 2. Changes in redox potentials and electronic transition energies are dominated by intramolecular electrostatic interactions, *J. Am. Chem. Soc. 120*, 3684−3693.
29. Cotton, A. A., and Wilkinson, G. (1988) *Advanced Inorganic Chemistry*, 5th ed., John Wiley & Sons, NewYork.
30. Evans, T. A., and Katz, J. J. (1975) Evidence for 5- and 6-coordinated magnesium in bacteriochlorophyll a from visible absorption spectroscopy, *Biochim. Biophys. Acta 396*, 414−426.
31. Callahan, P. M., and Cotton, T. M. (1987) Assignment of bacteriochlorophyll a ligation state from absorption and resonance Raman spectra, *J. Am. Chem. Soc. 109*, 7001−7007.
32. Sauer, K., Smith, J. R. L., and Schultz, A. J. (1966) The dimerization of chlorophyll a, chlorophyll b, and bacteriochlorophyll in solution, *J. Am. Chem. Soc. 88*, 2681−2688.
33. Ballschmiter, K., Truesdell, K., and Katz, J. J. (1969) Aggregation of chlorophyll in nonpolar solvents from molecular weight measurements, *Biochim. Biophys. Acta 184*, 604−613.
34. Katz, J. J., Shipman, L. L., Cotton, T. M., and Janson, T. J. (1978) Chlorophyll aggregation: Coordination interactions in chlorophyll monomers, dimers, and oligomers, in *The Porphyrins* (Dolphin, D., Ed.) pp 401−458, Academic Press, New York.
35. Balaban, T. S. (2003) Are syn-ligated (bacterio)chlorophyll dimers energetic traps in light-harvesting systems? *FEBS Lett. 545*, 97−102.
36. Oba, T., and Tamiaki, H. (2002) Which side of the π-macrocycle plane of (bacterio)chlorophylls is favored for binding of the fifth ligand? *Photosynth. Res. 74*, 1−10.
37. Katz, J. J., Strain, H. H., Leussing, D. L., and Dougherty, R. C. (1968) Chlorophyll-ligand interactions from nuclear magnetic resonance studies, *J. Am. Chem. Soc. 90*, 784−791.
38. Watanabe, T., and Kobayashi, M. (1991) Electrochemistry of chlorophylls, in *Chlorophylls* (Scheer, H., Ed.) pp 287−315, CRC Press, Boca Raton, FL.
39. Omata, T., and Murata, N. (1983) Preparation of chlorophyll a, chlorophyll b and bacteriochlorophyll a by column chromatography with DEAE-Sepharose CL-6B and Sepharose CL-6B, *Plant Cell Physiol. 24*, 1093−1100.
40. Watanabe, T., Hongu, A., Honda, K., Nakazato, M., Mazaki, H., Konno, M., and Saitoh, S. (1984) Preparation of chlorophylls and pheophytins by isocratic liquid chromatography, *Anal. Chem. 56*, 251−256.
41. Fiedor, L., Rosenbach-Belkin, V., and Scherz, A. (1992) The stereospecific interaction between chlorophylls and chlorophyllase. Possible implication for chlorophyll biosynthesis and degradation, *J. Biol. Chem. 267*, 22043−22047.
42. Fiedor, L., and Scheer, H. (2005) Trapping of an intermediate of LH1 complex assembly beyond the B820 subunit, *J. Biol. Chem. 280*, 20921−20926.
43. Picorel, R., Belanger, G., and Gingras, G. (1983) Antenna holochrome B880 of *Rhodospirillum rubrum* S1. Pigment, phospholipid, and polypeptide composition, *Biochemistry 22*, 2491−2497.
44. Fiedor, L., Akahane, J., and Koyama, Y. (2004) Carotenoid-induced cooperative formation of bacterial photosynthetic LH1 complex, *Biochemistry 43*, 16487−16496.
45. Kania, A., and Fiedor, L. (2005) Steric control of bacteriochlorophyll ligation, *J. Am. Chem. Soc. 128*, 454−458.
46. Scherz, A., and Rosenbach-Belkin, V. (1989) Comparative study of optical absorption and circular dichroism of bacteriochlorophyll oligomers in Triton X-100, the antenna pigment B850, and the primary donor P-860 of photosynthetic bacteria indicates that all are similar dimers of bacteriochlorophyll a, *Proc. Natl. Acad. Sci. U.S.A. 86*, 1505−1509.
47. Miller, J. F., Hinchigeri, S. B., Parkes-Loach, P. S., Callahan, P. M., Sprinkle, J. R., Riccobono, J. R., and Loach, P. A. (1987) Isolation and characterization of a subunit form of the light-harvesting complex of *Rhodospirillum rubrum*, *Biochemistry 26*, 5055−5062.
48. Permentier, H. P., Neerken, S., Overmann, J., and Amesz, J. (2001) A bacteriochlorophyll a antenna complex from purple bacteria absorbing at 963 nm, *Biochemistry 40*, 5573−5578.
49. Schwerzmann, R. U., and Bachofen, R. (1989) Carotenoid profiles in pigment−protein complexes of *Rhodospirillum rubrum*, *Plant Cell Physiol. 30*, 497−504.
50. Davis, C. M., Bustamante, P. L., and Loach, P. A. (1995) Reconstitution of the bacterial core light-harvesting complexes of *Rhodobacter sphaeroides* and *Rhodospirillum rubrum* with isolated α- and β-polypeptides, bacteriochlorophyll a, and carotenoid, *J. Biol. Chem. 270*, 5793−5804.
51. Akahane, J., Rondonuwu, F. S., Fiedor, L., Watanabe, Y., and Koyama, Y. (2004) Dependence of singlet-energy transfer on the conjugation length of carotenoids reconstituted into the LH1 complex from *Rhodospirillum rubrum* G9, *Chem. Phys. Lett. 393*, 184−191.

52. Umetsu, M., Wang, Z.-Y., Yoza, K., Kobayashi, M., and Nozawa, T. (2000) Interaction of photosynthetic pigments with various organic solvents 2. Application of magnetic circular dichroism to bacteriochlorophyll a and light-harvesting complex 1, *Biochim. Biophys. Acta 1457*, 106−117.
53. Küpper, H., Spiller, M., and Küpper, F. C. (2000) Photometric method for the quantification of chlorophylls and their derivatives in complex mixtures: Fitting with Gauss-peak spectra, *Anal. Biochem. 286*, 247−256.
54. Eichwurzel, I., Stiel, H., Teuchner, K., Leupold, D., Scheer, H., Salomon, Y., and Scherz, A. (2000) Photophysical consequences of coupling bacteriochlorophyll a with serine and its resulting solubility in water, *Photochem. Photobiol. 72*, 204−209.
55. Zucchelli, G., Jennings, R. C., Garlaschi, F. M., Cinque, G., Bassi, R., and Cremonesi, O. (2002) The calculated in vitro and in vivo chlorophyll a absorption bandshape, *Biophys. J. 82*, 378−390.
56. Kramer, H. J. M., Pennoyer, J. D., van Grondelle, R., Westerhuis, W. H. J., Niederman, R. A., and Amesz, J. (1984) Low-temperature optical properties and pigment organization of the B875 light-harvesting bacteriochlorophyll-protein complex of purple photosynthetic bacteria, *Biochim. Biophys. Acta 767*, 335−344.
57. Van Dorssen, R. J., Hunter, C. N., van Grondelle, R., Korenhof, A. H., and Amesz, J. (1988) Spectroscopic properties of antenna complexes of *Rhodobacter sphaeroides* in vitro, *Biochim. Biophys. Acta 932*, 179−188.
58. Law, C. J., and Cogdell, R. J. (1998) The effect of chemical oxidation on the fluorescence of the LH1 (B880) complex from the purple bacterium *Rhodobium marinum*, *FEBS Lett. 432*, 27−30.
59. Fiedor, L., Leupold, D., Teuchner, K., Voigt, B., Hunter, C. N., Scherz, A., and Scheer, H. (2001) Excitation trap approach to analyze size and pigment−pitment coupling: Reconstitution of LH1 antenna of *Rhodobacter sphaeroides* with Ni-substituted bacteriochlorophyll, *Biochemistry 40*, 3737−3747.
60. Qian, P., Yagura, T., Koyama, Y., and Cogdell, R. J. (2000) Isolation and purification of the reaction center (RC) and the core (RC-LH1) complex from *Rhodobium marinum*: The LH1 ring of the detergent-solubilized complex contains 32 bacteriochlorophylls, *Plant Cell Physiol. 41*, 1347−1353.
61. Jamieson, S. J., Wang, P., Qian, P., Kirkland, J. Y., Conroy, M. J., Hunter, C. N., and Bullough, P. A. (2002) Projection structure of the photosynthetic reaction centre-antenna complex of *Rhodospirillum rubrum* at 8.5 Å resolution, *EMBO J. 21*, 3927−3935.
62. Qian, P., Addlesee, H. A., Ruban, A. V., Wang, P., and Bullough, P. A. (2003) A reaction center-light-harvesting 1 complex (RC-LH1) from a *Rhodospirillum rubrum* mutant with altered esterifying pigments, *J. Biol. Chem. 278*, 23678−23685.
63. Gudowska-Nowak, E., Newton, M. D., and Fajer, J. (1990) Conformational and environmental effects on bacteriochlorophyll optical spectra: Correlations of calculated spectra with structural results, *J. Phys. Chem. 94*, 5795−5801.
64. Lapouge, K., Nveke, A., Gall, A., Ivancich, A., Seguin, J., Scheer, H., Sturgis, J. N., Matiolli, T. A., and Robert, B. (1999) Conformation of bacteriochlorophyll molecules in photosynthetic proteins from purple bacteria, *Biochemistry 38*, 11115−11121.
65. Cotton, T. M., and Van Duyne, R. P. (1981) Characterization of bacteriochlorophyll interactions in vitro by resonance Raman spectroscopy, *J. Am. Chem. Soc. 103*, 6020−6026.
66. Fujiwara, M., and Tasumi, M. (1986) Resonance Raman and infrared studies on axial coordinatioon of chlorophyll a and b in vitro, *J. Phys. Chem. 90*, 250−255.
67. Sturgis, J. N., and Robert, B. (1997) Pigment binding-site and electronic properties in light-harvesting proteins of purple bacteria, *J. Phys. Chem. B 101*, 7227−7231.
68. Näveke, A., Lapouge, K., Sturgis, J. N., Hartwich, G., Simonin, I., Scheer, H., and Robert, B. (1997) Resonance Raman spectroscopy of metal-substituted bacteriochlorophylls: Characterization of Raman bands sensitive to bacteriochlorin conformation, *J. Raman Spectrosc. 28*, 599−604.
69. Yerushalmi, R., Scherz, A., and Baldridge, K. K. (2004) Direct experimental evaluation of charge scheme performance by a molecular charge-meter, *J. Am. Chem. Soc. 126*, 5897−5905.
70. Krawczyk, S. (1989) The effects of hydrogen bonding and coordination interaction in visible absorption and vibrational spectra of chlorophyll a, *Biochim. Biophys. Acta 976*, 140−149.
71. Fenna, R. E., and Matthews, B. W. (1975) Chlorophyll arrangement in a bacteriochlorophyll protein from *Chlorobium limicola*, *Nature 258*, 573−577.
72. Fiedor, L., Rosenbach-Belkin, V., Sai, M., and Scherz, A. (1996) Preparation of tetrapyrrole-amino acid covalent complexes, *Plant Physiol. Biochem. 34*, 393−398.
73. Wang, Z.-Y., Gokan, K., Kobayashi, M., and Nozawa, T. (2005) Solution structures of the core light-harvesting α and β polypeptides from *Rhodospirillum rubrum*: Implications for the pigment−protein and protein−protein interactions, *J. Mol. Biol. 347*, 465−477.
74. Roszak, A. W., Howard, T. D., Southall, J., Gardiner, A. T., Law, C. J., Isaacs, N. W., and Cogdell, R. J. (2003) Crystal structure of the RC-LH1 core complex from *Rhodopseudomonas palustris*, *Science 302*, 1969−1972.
75. Gerken, U., Jelezko, F., Götze, B., Branschädel, M., Tietz, C., Ghosh, R., and Wrachtrup, J. (2003) Membrane environment reduces the accessible conformational space available to an integral membrane protein, *J. Phys. Chem. 107*, 338−343.
76. Fotiadis, D., Qian, P., Philippsen, A., Bullough, P. A., Engel, A., and Hunter, C. N. (2004) Structural analysis of the reaction center light-harvesting complex I photosynthetic core complex of *Rhodospirillum rubrum* using atomic force microscopy, *J. Biol. Chem. 279*, 2063−2068.
77. Bahatyrova, S., Frese, R. N., van der Werf, K. O., Otto, C., Hunter, C. N., and Olsen, C. N. (2004) Flexibility and size heterogeneity of the LH1 light harvesting complex revealed by atomic force microscopy, *J. Biol. Chem. 279*, 21327−21333.
78. Lapouge, K., Näveke, A., Robert, B., Scheer, H., and Sturgis, J. N. (2000) Exchanging cofactors in the core antennae from purple bacteria: Structure and properties of Zn-bacteriopheophytin-containing LH1, *Biochemistry 39*, 1091−1099.
79. Nagae, H., Kakitani, T., Katoh, T., and Mimuro, M. (1993) Calculation of the excitation transfer matrix elements between the S_2 or S1 states of carotenoid and the S_2 or S1 state of bacteriochlorophyll, *J. Chem. Phys. 98*, 8012−8023.
80. Ritz, T., Damjanovic, A., Schulten, K., Zhang, J.-P., and Koyama, Y. (2000) Efficient light harvesting through carotenoids, *Photosynth. Res. 66*, 125−144.
81. Macpherson, A. N., Arellano, J. B., Fraser, N. J., Cogdell, R. J., and Gillbro, T. (2001) Efficient energy transfer from the carotenoid S_2 state in a photosynthetic light-harvesting complex, *Biophys. J. 80*, 923−930.
82. Freer, A., Prince, S., Sauer, K., Papiz, M., Hawthornthwaite-Lawless, A., McDermott, G., Cogdell, R., and Isaacs, N. W. (1996) Pigment−pitment interactions and energy transfer in the antenna complex of the photosynthetic bacterium *Rhodopseudomonas acidophila*, *Structure 4*, 449−462.
83. Desamero, R. Z. B., Chynwat, V., van der Hoef, I., Jansen, F. J., Lugtenburg, J., Gosztola, D., Wasielewski, M. R., Cua, A., Bocian, D. F., and Frank, H. A. (1998) Mechanism of energy transfer from carotenoids to bacteriochlorophyll: Light-harvesting by carotenoids having different extents of π-electron conjugation incorporated into the B850 antenna complex from the carotenoidless bacterium *Rhodobacter sphaeroides* R-26.1, *J. Phys. Chem. B 102*, 8151−8162.

BI0514055